Physics Letters B 809 (2020) 135709

Contents lists available at ScienceDirect

Physics Letters B

www.elsevier.com/locate/physletb

Constraints on the coupling with photons of heavy axion-like-particles from Globular Clusters

Pierluca Carenza [a,b,*], Oscar Straniero [c], Babette Döbrich [d], Maurizio Giannotti [e], Giuseppe Lucente [a], Alessandro Mirizzi [a,b]

[a] Dipartimento Interateneo di Fisica "Michelangelo Merlin", Via Amendola 173, 70126 Bari, Italy
[b] Istituto Nazionale di Fisica Nucleare, Sezione di Bari, Via Orabona 4, 70126 Bari, Italy
[c] INAF, Osservatorio Astronomico d'Abruzzo, 64100 Teramo, Italy
[d] CERN, Esplanade des Particules 1, 1211 Geneva 23, Switzerland
[e] Physical Sciences, Barry University, 11300 NE 2nd Ave., Miami Shores, FL 33161, USA

ARTICLE INFO

Article history:
Received 28 April 2020
Received in revised form 27 July 2020
Accepted 17 August 2020
Available online 26 August 2020
Editor: A. Ringwald

ABSTRACT

We update the globular cluster bound on massive (m_a up to a few 100 keV) axion-like particles (ALP) interacting with photons. The production of such particles in the stellar core is dominated by the Primakoff $\gamma + Ze \to Ze + a$ and by the photon coalescence process $\gamma + \gamma \to a$. The latter, which is predominant at high masses, was not included in previous estimations. Furthermore, we account for the possibility that axions decay inside the stellar core, a non-negligible effect at the masses and couplings we are considering here. Consequently, our result modifies considerably the previous constraint, especially for $m_a \gtrsim 50$ keV. The combined constraints from Globular Cluster stars, SN 1987A, and beam-dump experiments leave a small triangularly shaped region open in the parameter space around $m_a \sim 0.5 - 1$ MeV and $g_{a\gamma} \sim 10^{-5}$ GeV^{-1}. This is informally known as the ALP "cosmological triangle" since it can be excluded only using standard cosmological arguments. As we shall mention, however, there are viable cosmological models that are compatible with axion-like particles with parameters in such region. We also discuss possibilities to explore the cosmological triangle experimentally in upcoming accelerator experiments.

1. Introduction

Axion-like-particles (ALPs) with masses m_a in the keV-MeV range emerge in different extension of the Standard Model, as Pseudo-Goldstone bosons of some broken global symmetry. The theoretical speculation about *superheavy* axion models began long ago (see Sec. 6.7 of Ref. [1] for a recent review), in an attempt to get rid of the strong astrophysical bounds on the axion coupling, which made it effectively invisible. In this context, superheavy means heavier than about 100 keV, so that the axion production in most stars (supernovae and neutron stars being an exception) is Boltzmann suppressed and the majority of the stellar axion bounds are relaxed. Nowadays, several mechanisms exist to increase the axion mass independently from its couplings, without spoiling the solution of the strong CP problem (a list of references can be found in [1]).

Besides QCD axions, heavy ALPs emerge in compactification scenarios of string theory [2–4], or in the context of "relaxion" models [5]. Heavy ALPs have also recently received considerable attention in the context of Dark Matter model-building. Indeed, they may act as mediators for the interactions between the Dark Sector and Standard Model (SM) allowing to reproduce the correct Dark Matter relic abundance via thermal freeze-out [6,7]. ALPs with masses below the MeV scale can have a wide range of implications for cosmology and astrophysics (see [8] for a review), affecting for example Big Bang Nucleosynthesis (BBN), the Cosmic Microwave Background (CMB) [9–11] and the evolution of stars. Colliders and beam-dump experiments are also capable to explore this mass range, indeed reaching the $m_a \sim \mathcal{O}$ (GeV) frontier, which is not covered by any astrophysical or cosmological considerations [8,12,13].

In this work we are interested in ALPs interacting exclusively with photons. Additional couplings with SM fields, particularly with electrons, may spoil some of our conclusions. For such ALPs, the collection of all the astrophysical and experimental constraints

* Corresponding author.
E-mail address: pierluca.carenza@ba.infn.it (P. Carenza).

https://doi.org/10.1016/j.physletb.2020.135709

leaves a triangular area in the parameter space, for masses $m_a \sim 0.5 - 1$ MeV and couplings $g_{a\gamma} \sim 10^{-5}$ GeV^{-1}, open. Although the existence of ALPs with such parameters is in tension with standard cosmological arguments [9,10], the region of such masses and couplings passes the current experimental tests and all the known astrophysical arguments, and is also permitted in viable non-standard cosmological scenarios [11]. Because of that, this parameter area is sometimes dubbed as the ALP *"cosmological triangle"*. As we shall discuss in Sec. 5, this region is now the target of several direct investigations, as more and more experiments are reaching the sensitivity to probe those masses and couplings, and there is a chance that such area might be covered in the next decade or so. Redefining the boundaries of the cosmological triangle is, therefore, particularly timely and relevant to guide the experimental investigations.

In this work we revisit the globular cluster bound on heavy ALPs, which defines the low-mass boundary of the cosmological triangle. Globular Clusters (GC) are gravitationally bound systems of stars, typically harboring a few millions stars. Being among the oldest objects in the Milky Way, their population is made of low-mass stars ($M < 1 M_\odot$). Most of these stars belong to the so-called Main Sequence, which corresponds to the H burning evolutionary phase. However, there are two other well defined evolutionary phases, i.e., the Red Giant Branch (RGB) and the Horizontal Branch (HB). The first is made by cool giant stars, burning H in a thin shell surrounding a compact He-rich core. During the RGB phase the stellar luminosity increases and the core contracts, until the temperature rises enough to ignite He. Then, stars leave the RGB and enter the HB phase, during which they burn He, in the core, and H, in the shell.

The number of stars found in the different evolutionary phases depends linearly on the time spent by a star in each of them. For this reason, stellar counts provide a powerful tool to investigate the efficiency of the energy sources and sinks in stellar interiors, those that affect the stellar lifetime τ in a given stage of the stellar evolution. In this context, the GC R parameter, defined as the number ratio of horizontal branch to red giants branch stars, i.e.:

$$R = \frac{N_{\rm HB}}{N_{\rm RGB}} = \frac{\tau_{\rm HB}}{\tau_{\rm RGB}}, \tag{1}$$

is a powerful observable often used to investigate stellar physics. In particular, it has been also exploited to constrain the axion-photon coupling $g_{a\gamma}$ [19–22], at least for ALPs light enough, $m_a \lesssim 30$ keV, that their production is not Boltzmann suppressed. At such low masses, the most relevant axion production mechanism induced by the photon coupling is the Primakoff process, $\gamma + Ze \to Ze + a$, i.e. the conversion of a photon into an ALP in the electric field of nuclei and electrons in the stellar plasma (cf. Sec. 2). This process is considerably more efficient in HB than in RGB stars, since in the latter case it is suppressed due to the larger screening scale and plasma frequency (see Sec. 2). Therefore, the energy-loss caused by the production of ALPs with a sizable $g_{a\gamma}$ would imply a reduction of the HB lifetime and, in turn, a reduction of the R parameter. As it turns out, R has a substantial dependence, approximately linear, on the helium abundance of the cluster and, if ALPs are also included, a quadratic dependence on the axion-photon coupling. On the other hand, the R parameter is only marginally affected by a variation of the cluster age and metallicity. Thus, once the He abundance is known from direct or indirect measurements, bounds (or hints) on the axion-photon coupling can be obtained from the comparison of the R parameter measured in Globular clusters with the theoretical expectations obtained by varying $g_{a\gamma}$ [21–24]. An accurate application of this method, based on photometric data for 39 GCs, was discussed in [21] by some of us, who found an upper bound $g_{a\gamma} < 0.66 \times 10^{-10}$ GeV^{-1} at 95% confidence level, a value more recently experimentally confirmed by the CAST collaboration [25].

The goal of the present work is to extend the GC bound on $g_{a\gamma}$ to higher axion masses. Given the typical temperature $T \sim 10$ keV in the stellar core of a HB star, one expects the thermal production of particles to be Boltzmann suppressed for $m_a \gtrsim 30$ keV, relaxing the bound on $g_{a\gamma}$. A quantitative analysis was carried out in [10], where a bound was derived from the requirement that the axion energy emitted per unit time and mass, ε_a, averaged over a typical HB core, satisfies the requirement $\langle \varepsilon_a \rangle \lesssim 10\,{\rm erg\,g^{-1}\,s^{-1}}$ [26]. However, that analysis neglected the contribution of the photon coalescence process $\gamma\gamma \to a$ (cf. Sec. 2), to the ALP production in stars. At low masses, this process is subdominant and it is forbidden for $m_a < 2\,\omega_{\rm pl}$, where $\omega_{\rm pl}$ is the plasma frequency at the position where the process takes place. Hence, the inclusion of the photon coalescence does not affect the bound obtained in Ref. [21], which remains valid for light axions ($m_a \lesssim 10$ keV). As we shall show in Sec. 2, however, for masses $m_a \gtrsim 50$ keV, the coalescence production dominates and becomes several times larger than the Primakoff at masses $\gtrsim 100$ keV. Furthermore, ALPs with a large mass and coupling have a non-negligible probability to decay inside the stellar core. In this case, they would not contribute to the cooling of the star. We show that this is the case for the couplings and masses within the cosmological triangle and conclude that the stellar bounds in this region are considerably relaxed with respect to what shown in the previous literature.

The plan of our work is the following. In Sec. 2, we revise the axion emissivity via the Primakoff conversion and the photon coalescence. In Sec. 3, we discuss our procedure and present our bound on $g_{a\gamma}$ for massive ALPs. Then, we show the complementarity of our bound with other constraints. In Sec. 4, with that from SN 1987A (in the trapping regime), and in Sec. 5 with the experimental bounds from beam-dump searches. Finally, in Sec. 6 we summarize our results and we conclude. In Appendix A we compute the photon-axion transition rate from Primakoff conversion and in Appendix B we calculate the ALP production rate from Primakoff conversion and photon coalescence.

2. Axion emissivity

The ALP-two photon vertex is described by the Lagrangian term

$$\mathcal{L}_{a\gamma} = -\frac{1}{4}\, g_{a\gamma}\, F_{\mu\nu} \tilde{F}^{\mu\nu} a = g_{a\gamma}\, \mathbf{E}\cdot\mathbf{B}\, a\,, \tag{2}$$

where $g_{a\gamma}$ is the ALP-photon coupling constant (which has dimension of an inverse energy), F the electromagnetic field and $\tilde{F}$ its dual.

The primary production mechanisms for ALPs interacting with *transverse* photons in the core of a HB star are:

- the Primakoff conversion $\gamma + Ze \to Ze + a$, where a thermal photon in the stellar core converts into an axion in the Coulomb fields of nuclei and electrons;
- the photon coalescence process $\gamma\gamma \to a$, where two photons in a medium of sufficiently high density annihilate producing an axion.

As we shall see, the former dominates at low ALP masses ($m_a \lesssim 50$ keV) while at large mass the photon coalescence takes over.

There is a vast literature on the axion Primakoff conversion rate. The interested reader may consult Ref. [10,19] for a detailed discussion. Here, we provide only a brief review and present some results applicable in the typical plasma conditions relevant for this work. In general, the axion emission rate (energy per mass per time) via the Primakoff conversion is given by the expression

$$\varepsilon_a = \frac{2}{\rho}\int \frac{dk\,k^2}{2\pi^2}\Gamma_{\gamma\to a}\,E\,f(E)\ , \tag{3}$$

where the factor 2 comes from the photon degrees of freedom, ρ is the local density, $f(E) = (e^{E/T}-1)^{-1}$ is the Bose-Einstein distribution, and $\Gamma_{\gamma\to a}$ is the photon-axion transition rate,

$$\Gamma_{\gamma\to a} = \frac{g_{a\gamma}^2 T\kappa^2}{32\pi}\frac{p}{E}\left\{\frac{[(k+p)^2+\kappa^2][(k-p)^2+\kappa^2]}{4pk\kappa^2}\right.$$
$$\ln\left[\frac{(k+p)^2+\kappa^2}{(k-p)^2+\kappa^2}\right]$$
$$\left.-\frac{(k^2-p^2)^2}{4kp\kappa^2}\ln\left[\frac{(k+p)^2}{(k-p)^2}\right]-1\right\}\ . \tag{4}$$

In the last expression, E and $p=\sqrt{E^2-m_a^2}$ are, respectively, the ALP energy and momentum. The photon obeys the dispersion relation $k=\sqrt{\omega^2-\omega_{\rm pl}^2}$ where k is the photon momentum, ω its energy, and $\omega_{\rm pl}^2 \simeq 4\pi\alpha n_e/m_e$ is the plasma frequency (or effective "photon mass"). In a photon-axion transition the energy is conserved because we ignore recoil effects. Therefore, we use $\omega = E$. Finally κ is the screening scale

$$\kappa^2 = \frac{4\pi\alpha}{T}\left(n_e^{\rm eff}+\sum_j Z_j^2 n_j^{\rm eff}\right)\ , \tag{5}$$

where $n_e^{\rm eff}$ and $n_j^{\rm eff}$ are, respectively, the effective number of electrons and ions with nuclear charge $Z_j e$. Note that in the center of a HB star, $T\sim 8.6$ keV, $\rho\sim 10^4$ g cm^{-3}, and $\omega_{\rm pl}\sim 3$ keV. Thus, the plasma frequency is considerably smaller than the thermal energy. Nevertheless, to achieve a higher accuracy our numerical Primakoff emission rate includes also the effects induced by a finite plasma frequency (a detailed description of the adopted emission rate can be found in the Appendix of Ref. [28], which we have generalized at finite ALP mass).

The axion coalescence process, $\gamma\gamma\to a$, has a kinematic threshold, vanishing for $m_a \le 2\omega_{\rm pl}$ [29]. As we shall see, above this threshold the production rate is a steep function of the mass and dominates over the Primakoff at $m_a \gtrsim 50$ keV. In order to calculate the axion coalescence rate in a thermal medium, it is convenient to approximate the Bose-Einstein photon distribution with a Maxwell-Boltzmann, $f(E)\to e^{-E/T}$, for the photon occupation number [29]. This approximation is justified since we are interested only in axion masses (and thus axion energies) of the order of the temperature or larger (for $m_a \lesssim T$ the coalescence process is practically negligible). As shown in Appendix B, the production rate per unit volume of ALPs of energy between E and $E+dE$ is [29]

$$d\dot{N}_a = \frac{g_{a\gamma}^2 m_a^4}{128\pi^3}p\left(1-\frac{4\omega_{\rm pl}^2}{m_a^2}\right)^{3/2} e^{-E/T}dE\ , \tag{6}$$

and the axion emissivity (per unit mass):

$$\varepsilon_a = \frac{1}{\rho}\int E\frac{d\dot{N}_a}{dE}dE\ . \tag{7}$$

The temperature and density profiles within the He-rich core of a typical HB stellar model are shown in Fig. 1. The model has been evolved starting from the pre-main sequence up to the end of the core He burning phase. For the initial structure ($t=0$ model) we have adopted a mass M $= 0.82\ M_\odot$ and, as usual, a homogeneous composition, namely: $Y=0.25$ and $Z=0.001$. After ~ 13 Gyr the central He burning begins (zero age HB). At that time the stellar mass is $m\sim 0.72\ M_\odot$, while the mass of the He-rich core is $m\sim 0.5\ M_\odot$. Fig. 1 is a snapshot of the stellar core taken when the central mass fraction of He reduces down to $X_{He}\sim 0.6$. The corresponding Primakoff and photon coalescence emission rates are compared in Fig. 2. The quantity reported in the vertical axis is the ratio of the energy-loss rate, in units of erg g^{-1} s^{-1}, and the square of the axion-photon coupling, $g_{10}\equiv g_{a\gamma}/10^{-10}$ GeV^{-1}. The Primakoff and photon coalescence emission rates have been computed for two different values of the axion mass, namely: $m_a = 30$ keV and $m_a = 80$ keV. In the case of $m_a = 30$ keV, the Primakoff energy-loss rate (in the center of the star) is a factor of ~ 3 larger than the photon coalescence rate. Conversely, for $m_a = 80$ keV the photon coalescence dominates and the contribution of the Primakoff is effectively negligible.

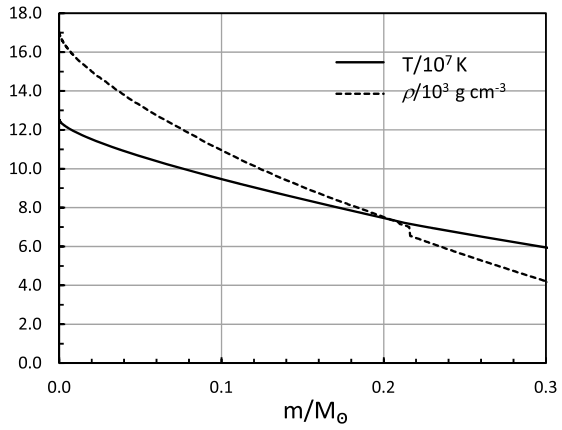

Fig. 1. Profiles of temperature T (solid line) and density ρ (dotted line) within the core of typical HB star (see text for details). The most internal 0.3 $M_\odot$ are shown.

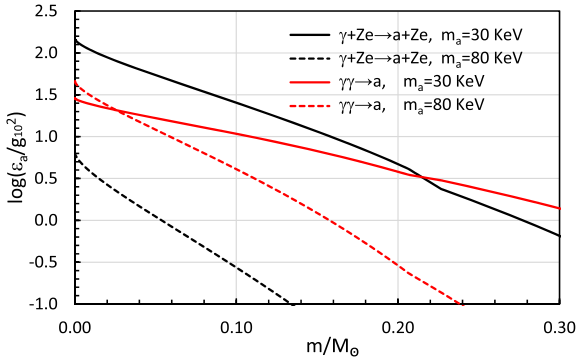

Fig. 2. Energy-loss rates (in units of erg g^{-1} s^{-1} and normalized for $g_{10}=1$) for Primakoff ($\gamma + Ze\to a+Ze$) and photon coalescence ($\gamma\gamma\to a$) within the core of a typical HB star. The most internal 0.3 $M_\odot$ is shown. This is the same model used for Fig. 1. Results for two different axion mass, $m_a = 30$ keV and $m_a = 80$ keV, are shown.

Fig. 3 shows how the ALP luminosity,

$$L_a = 4\pi\int \rho\varepsilon_a r^2 dr\ , \tag{8}$$

depends on the ALP mass m_a. The integration is extended from the center ($r=0$) to the stellar surface. According to our expectations, the coalescence process is sub-leading for $m_a \lesssim 50$ keV, but it dominates at higher masses. Note that the stellar luminosity, as due to the photon emission, is $L\sim 2\times 10^{35}$ erg s^{-1}, which is about 2 orders of magnitude larger than the axion luminosity at $g_{10}\sim 1$.

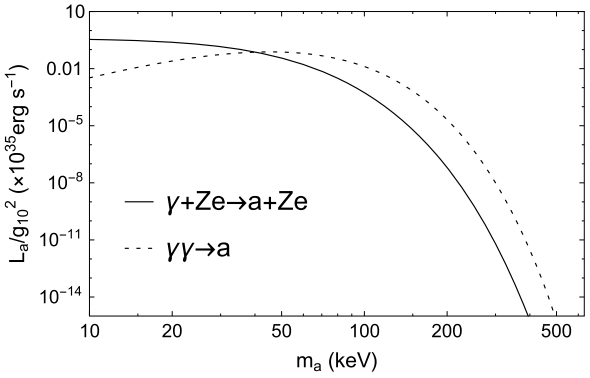

Fig. 3. ALP luminosity for Primakoff process ($\gamma + Ze \to a + Ze$, continuous curve) and for photon coalescence ($\gamma\gamma \to a$, dashed curve) versus axion mass m_a. The HB model is the one used in Fig. 1. As for the rates in Fig. 2, the luminosities are normalized to $g_{10} = 1$.

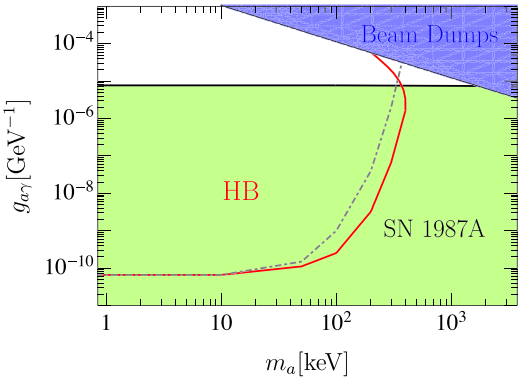

Fig. 4. HB bound (red line) in the plane $g_{a\gamma}$ *vs* m_a, compared with other exclusion limits. The dashed gray curve presents the HB limit accounting only for Primakoff while the continuous red curve includes also the photon coalescence process.

3. Globular cluster bound

In order to derive a bound on $g_{a\gamma}$ for massive ALPs, we have computed several evolutionary sequences of stellar models, from the pre-main-sequence to the end of the core He burning. The models have been computed by means of FuNS (Full Network Stellar evolution), an hydrostatic 1D stellar evolution code [28]. In general, the inclusion of the axion energy-loss in stellar model computations leads to a reduction of the R parameter, defined in Eq. (1). On the other hand, the larger the initial He abundance the larger the estimated R. In practice, the upper bound on the axion-photon coupling is obtained when the largest possible value of the He abundance is assumed. Analyzing the He abundance measured in molecular clouds with metallicity in the same range of those of galactic GCs, in Ref. [21] it was estimated a conservative upper limit for the He abundance, specifically $Y = 0.26$. Adopting this value of Y, it was shown that the R parameter obtained from photometric observations of 39 GCs, $R = 1.39 \pm 0.03$, implies the stringent upper bound $g_{a\gamma} = 0.66 \times 10^{-10}\,\text{GeV}^{-1}$ (95% C.L.). However, this bound is only valid for light axions.

Since ALPs interacting only with photons are not efficiently produced in the core of RGB stars, and hence affect minimally the RGB lifetime (τ_{RGB} in Eq. (1)), the variation of R due to an axion production is essentially a consequence of the reduction of the HB lifetime (τ_{HB} in Eq. (1)). We have computed τ_{HB} for a GC benchmark. Specifically, we used: age 13 Gyr, metallicity $Z = 0.001$, and $Y = 0.26$, corresponding to the conservative upper limit for the GC He abundance reported in [21]. In the standard case, when no exotic energy-loss process is included, we found $\tau_{HB} = 8.84 \times 10^7$ yr. The addition of light axions with $g_{a\gamma} = 0.66 \times 10^{-10}$ GeV^{-1} reduces the HB lifetime down to $\tau_{HB} = 7.69 \times 10^7$ yr. Requiring the HB lifetime to be within these values guarantees that the predicted R parameter is consistent, within 2σ, with the observed one.

The argument was generalized to massive ALPs by searching for the ALP-photon coupling that reduces the HB lifetime down to $\tau_{HB} = 7.69 \times 10^7$ yr at each fixed ALP mass. Notice that the ALP decay length decreases rapidly with the ALP mass and coupling,

$$\lambda_a = 5.7 \times 10^{-5}\ g_{10}^{-2} m_{\text{keV}}^{-3} \frac{\omega}{m_a} \sqrt{1 - \left(\frac{m_a}{\omega}\right)^2} R_\odot\ , \tag{9}$$

with $m_{\text{keV}} = m_a/(1\ \text{keV})$. Thus, for the masses and couplings we are interested in, a considerable fraction of ALPs may decay inside the star. Those ALPs do not contribute to energy loss, but they can lead to an efficient energy transfer inside the star [30]. In order to address this issue one should perform a dedicated simulation of HB evolution including ALP energy transfer. This is a challenging task that we leave for a future work. For the moment we adopt a conservative approach assuming that the ALPs decaying inside the *convective* core, with a radius $R_c \simeq 3 \times 10^{-2} R_\odot$, do not lead to any energy transfer, convection being a very efficient energy transfer mechanism by itself. Neglecting the contribution of these ALPs leads to the deterioration of the ALP bound that we observe for $g_{a\gamma} \gtrsim 10^{-6}$ GeV^{-1}. Our result remains effectively unchanged if we replace the convective core with the entire Helium core, $R \simeq 7 \times 10^{-2} R_\odot$, as our threshold radius. We stress, however, that our bound might relax even further if a detailed simulation were to show that even ALPs decaying at larger radii are inefficient in transferring energy. Our result is shown in the exclusion plot reported in Fig. 4. The continuous red line indicates our new result (95% C.L.) while the dashed gray line represents the bound ignoring the coalescence production and the ALP decay, and corresponds roughly to the previous constraint. It is evident how the bound loses its strength for masses above ~ 30 keV, because of the Boltzmann suppression of the axion emissivity.

For such high masses one may ask if ALPs can be gravitationally trapped into the star gravitational field. In this case ALPs escape only if their kinetic energy is greater than

$$U(r) = \frac{G M_r m_a}{r} = 7.44 \times 10^{-34} \text{keV} \frac{M_r}{\text{g}} \frac{m_a}{\text{keV}} \frac{\text{km}}{r}\ ; \tag{10}$$

where M_r is the star mass up to the radius r and m_a is the ALP mass. As a simple estimate we consider the border of the core, outside the gravitational potential well is weaker. Therefore we use $M_r = 10^{33}$ g, $r = 5 \times 10^4$ km and $m_a = 500$ keV obtaining $U(r) = 8 \times 10^{-3}$ keV which is much smaller than the typical temperature $T \sim 10$ keV. In conclusion this effect is negligible.

For reference, in the figure we are also showing, in light green, the region excluded by SN 1987A in the regime of ALPs trapped in the SN core (see Sec. 4), and in blue the parameters excluded by direct searches at beam dump experiments (see Sec. 5). Interestingly, the combination of all the astrophysical and experimental bounds leaves a small triangular area, roughly at $m_a \sim 0.5 - 1$ MeV and $g_{a\gamma} \sim 10^{-5}$ GeV^{-1}, unconstrained. This is the ALP cosmological triangle. Standard cosmological arguments, particularly concerning BBN and the allowed effective number of relativistic species, N_{eff}, can be used to exclude this area [10,11]. Nevertheless, in non-standard cosmological scenarios, e.g. in low-reheating models, the cosmological bounds can be relaxed all the way to the GC bound calculated in this work [11]. Thus, the cosmological triangle is still a viable region of the ALP parameter space, open to experimental and phenomenological investigations.

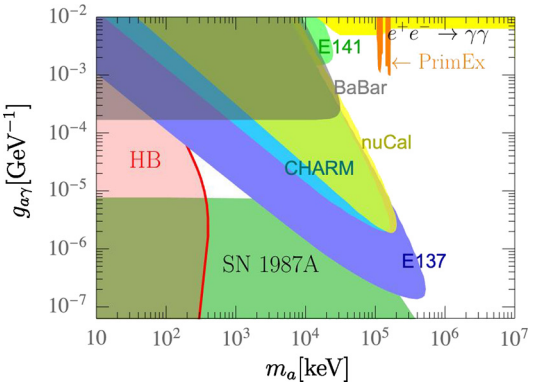

Fig. 5. Overview of the heavy ALP parameter space in the plane $g_{a\gamma}$ *vs* m_a. The red-filled region labeled "HB" represents our new exclusion result. The SN 1987A bound [32] and the experimental limits, compiled from Refs. [8,13], are also shown. Prospects to experimentally probe the viable region are commented on in the text.

4. SN 1987A bound from axion trapping

For the sake of completeness, in this section we present briefly our derivation of the SN 1987A constraint on heavy ALPs presented in Fig. 4 and 5. A detailed study of this constraint, based on state-of-the-art SN models [31], is currently ongoing and will be the topic of a forthcoming work by some of us [32]. Here, we just present a succinct discussion of the SN argument to constraint the ALP-photon couplings at the bottom edge of the cosmological triangle. In order to characterize the ALP emissivity in a SN, and in particular the effect of degeneracy in a SN core we closely follow [33].

Heavy ALPs can be copiously produced in a supernova (SN) core via Primakoff and coalescence processes. Due to the higher core temperature, $T \sim \mathcal{O}(30)$ MeV, SNe can be used to probe ALP masses considerably larger than those probed by GCs (see, e.g. [8,34,35]). For couplings of interest in this work, $g_{a\gamma} \sim \mathcal{O}(10^{-5})$ GeV^{-1}, ALPs would be trapped in the SN, having a mean-free path smaller than the size of the SN core ($R \sim 10$ km) [8,34]. In this case, ALPs may contribute significantly to the energy transport in the star, modifying the SN evolution. Since SN 1987A neutrino data are in a reasonable agreement with core-collapse SN models without the emission of exotic species, one should require that ALPs interact more strongly than the particles which provide the standard mode of energy transfer, i.e. neutrinos.

When ALPs interact strongly enough to be trapped in the SN core, they are emitted from an *axion-sphere*, a spherical shell whose radius r_a is fixed by the optical depth being about unity. More specifically, we calculated r_a imposing that the optical depth

$$\tau_a = \int_{r_a}^{+\infty} \kappa_a \rho dr \ , \tag{11}$$

where κ_a is the axion opacity, satisfies the condition $\tau_a(r_a) \simeq 2/3$. This is analogous to the neutrino last scattering surface, i.e. the "neutrino-sphere", with radius r_ν.

Trapped ALPs have a black-body emission with a luminosity $L_a \propto r_a^2 T^4(r_a)$. In order to obtain the bound on $g_{a\gamma}$ one should impose [26,27]

$$L_a \lesssim L_\nu \ . \tag{12}$$

We are concerned mostly with a time posterior to 0.5–1 s, where the outer core has settled and the shock has begun to escape. Specifically, in our numerical calculation we refer to the SN model used in [36], for a representative post-bounce time $t_{\rm pb} = 1$ s.

We calculated the ALP opacity following the prescriptions in [30] (see [35] for an alternative approach). For masses $m_a \lesssim$ a few MeV, the dominant contribution to the axion opacity is due to the inverse Primakoff conversion, $a + Ze \to \gamma + Ze$,

$$\kappa_{a\to\gamma} = \frac{1}{\rho \lambda_{a\to\gamma}} = \frac{1}{\rho} \frac{\Gamma_{a\to\gamma}}{\beta_E} \ , \tag{13}$$

where $\lambda_{a\to\gamma}$ is the mean free-path, and $\beta_E = (1 - m_a^2/E^2)^{1/2}$. The inverse Primakoff conversion rate is $\Gamma_{a\to\gamma} = 2\Gamma_{\gamma\to a}$, with $\Gamma_{\gamma\to a}$ given in Eq. (4).

From $\kappa_{a\to\gamma}$ one can calculate the mean ALP Rosseland opacity [26]

$$\kappa_a^{-1} = \frac{\int_{m_a}^{\infty} \kappa_{a\to\gamma}^{-1} \beta_E \partial_T B_E dE}{\int_{m_a}^{\infty} \beta_E \partial_T B_E dE} \ , \tag{14}$$

where

$$B_E = \frac{1}{2\pi^2} \frac{E^2 (E^2 - m_a^2)^{1/2}}{e^{E/T} - 1} \ , \tag{15}$$

is the ALP thermal spectrum.

We derived our bound on axion coupling from the luminosity condition in Eq. (12), taking the axion-sphere radius that satisfies Eq. (11). As shown in Fig. 4, for $m_a < 10$ MeV, the luminosity condition excludes the values of the photon-axion coupling $g_{a\gamma} \lesssim 8 \times 10^{-6}$ GeV^{-1}, in agreement with previous results [8,34].

Note that the SN 1987A bound should not be considered at the same level of confidence as the GCs one, since it is not based on a self-consistent SN simulations. Performing such a simulation, which should include also the trapped ALPs, would be a challenging task (see, e.g., [37] for a recent investigation in the context of dark photons), and demand a separated investigation.

5. Direct experimental tests of the cosmological triangle

As discussed above, the ALP region at masses of a few MeV is the target of numerous investigations. In this section, we briefly comment on the existing experimental limits near the cosmological triangle and future prospects to test that region directly in experiments.

Fig. 5 shows an overview plot of the status of the search for heavy ALPs with our updated bound as discussed in this work in red, labeled "HB". Colored regions are excluded at 95% C.L. Other limits are compiled from references [8,13] and detailed therein. The experimental limits which are "nose-like-shaped" (E137 [38], CHARM [14], nuCal [15,16], E141 [17,18]) are from beam-dump setups, in which the ALP needs to live long enough to reach the detection volume (boundary at "large" couplings and masses). However, it should not be so long-lived that it can excape from it (boundary at "small" couplings and masses).

The most efficient experiment to "touch" the cosmic triangle was E137, shown as a blue-shaded region in Fig. 4. This bound is based on data published by the experiment E137 [38] and its revisit in [8]: around 2×10^{20} electrons were dumped into an aluminum target, potentially yielding to Primakoff-production of ALPs. However, no excess of expected photon signals was observed at a distance of ~ 200 m, leading to an exclusion limit.

The small-coupling-limit of E137 relevant for us in this context is largely determined by how *long-lived* ALPs can be while still being detected by the experiment. The limit estimated [8] for this reason seems robust as late ALP decays will suffer little from their non-negligible probability of showering in air. We thus show this limit in Fig. 5. Roughly spoken, a long baseline together with a relatively soft ALP spectrum (compared to proton dumps whose lower limits are at much larger couplings [13]), made E137 an ideal

fixed-target in probing the cosmological triangle at the top section of its parameter space.

As for the possibilities to probe the remaining region at $m_a \sim 1$ MeV, Ref. [8] details on prospects to significantly probe the cosmic triangle at Belle-II at a statistics of 50 ab^{-1}. Sensitivity is also expected at "active" beam dumps such as LDMX-type set-ups, that can infer the presence of ALPs through a "missing-momentum signature" [39]. The running experiment PADME, at Frascati, does not currently have the potential to reach the cosmological triangle [40,41] but could be potentially sensitive to this area after a luminosity upgrade.

It is worth stressing that far more experimental options to probe this triangle exist if the axion-coupling is not limited strictly to *direct* photon couplings [35]. However, this possibility is outside the assumptions made in our work.

6. Discussions and conclusions

In this work we have extended the GCs bound on the ALP-photon coupling to masses $m_a \gtrsim 10$ keV, in the region of the parameter space where the Boltzmann suppression of the axion emission rate can no longer be neglected. Our analysis improves on the previous work by including the coalescence process, $\gamma + \gamma \to a$, which is the dominating axion production mechanism at masses above ~ 50 keV, and by accounting for ALPs decaying inside the stellar core. The bound is shown in Fig. 4 (red line), where we also compare it to the bound obtained ignoring the ALPs decay and the coalescence process (dashed gray line). The inclusion of the coalescence reduced the allowed value of the axion photon coupling by a factor of ~ 4 at masses ~ 100 keV, and by over an order of magnitude at $m_a \gtrsim 200$ keV. At large masses and couplings, the ALP energy loss mechanism is hampered by ALPs decaying inside the stellar core and the axion bounds starts to relax. Quite interestingly, this effect becomes important very close to the edge of the cosmological triangle, opening up the region to future experimental probes.

Though excluded by standard cosmological arguments, the cosmological triangle is a viable region in non-standard cosmological scenarios, e.g. in low-reheating models, which relax substantially the cosmological bounds [11]. Thus, it remains an area of great experimental interest, as shown in our Fig. 5. Indeed, several theoretical models permit ALPs (and even QCD axions) with parameters in this region, as discussed in Sec. 1, making this a possible target area for future experimental investigations. Interestingly, a detection of an axion signal in this region would have dramatic cosmological consequences, requiring non-standard cosmological scenarios. This intriguing possibility confirms once more the nice complementarity between astrophysical, cosmological arguments and direct searches in order to corner or luckily discover axion-like-particles.

Declaration of competing interest

The authors declare that they have no known competing financial interests or personal relationships that could have appeared to influence the work reported in this paper.

Acknowledgements

We would like to thank Felix Kahlhoefer for helpful discussions. We are also grateful to the anonymous referee for important comments concerning the role of ALP decays inside the star. For this work, O.S has been funded by the Italian Space Agency (ASI) and the Italian National Institute for Astrophysics (INAF) under the agreement n. 2017-14-H.0 -attività di studio per la comunità scientifica di Astrofisica delle AlteEnergie e Fisica Astroparticellare. The work of P.C. and A.M. is partially supported by the Italian Instituto Nazionale di Fisica Nucleare (INFN) through the "Theoretical Astroparticle Physics" project and by the research grant number 2017W4HA7S, "NAT-NET: Neutrino and Astroparticle Theory Network" under the program PRIN 2017 funded by the Italian Ministero dell'Università e della Ricerca (MUR). B.D. acknowledges support through the European Research Council (ERC) under grant ERC-2018-StG-802836 (AxScale).

Appendix A. Photon-axion transition rate from Primakoff conversion

The differential rate for the Primakoff conversion is

$$d\Gamma_{\gamma\to a} = |\overline{\mathcal{M}}|^2 \frac{V}{T}\frac{d^3\mathbf{p}}{(2\pi)^3}\,, \tag{A.1}$$

where V is the normalization volume, T the interaction time and $|\overline{\mathcal{M}}|^2$ is the squared matrix element averaged over the initial photon polarization,

$$|\overline{\mathcal{M}}|^2 = \frac{1}{2}|\mathcal{M}|^2 = \frac{1}{2}\left| < a| \int dt d^3\mathbf{r}\, g_{a\gamma}\, \phi_a\, \mathbf{E}_e \cdot \mathbf{B}|\gamma > \right|^2 , \tag{A.2}$$

where ϕ_a, $\mathbf{B}$ and $\mathbf{E}_e = \frac{Ze\mathbf{r}}{|\mathbf{r}|^3}$ are the interacting fields. By expanding the axion field ϕ_a and the magnetic field $\mathbf{B}$ in plane waves, one obtains

$$|\overline{\mathcal{M}}|^2 = \frac{1}{2}\left(\frac{g_{a\gamma} Ze}{2V}\right)^2 \frac{|\mathbf{k}\times\mathbf{p}|^2}{|\mathbf{k}-\mathbf{p}|^4}\frac{2\pi T\delta(\omega_k - \omega_p)}{\omega_k\omega_p}\,. \tag{A.3}$$

Therefore the transition rate results to be

$$\Gamma_{a\to\gamma} = \frac{1}{2V}\left(\frac{g_{a\gamma} Ze}{4\pi}\right)^2 \frac{|\mathbf{k}\times\mathbf{p}|^2}{|\mathbf{k}-\mathbf{p}|^4}\frac{|\mathbf{p}|}{E}\, d\Omega_p\,, \tag{A.4}$$

where $E = \omega_k = \omega_p$ because of the delta function in Eq. (A.3) and Ω_p is the scattering angle.

One has to consider that in a real plasma the particles mutually interact through their Coulomb fields and their motion is slightly correlated. This correlation implies the substitution [42]

$$\frac{1}{|\mathbf{k}-\mathbf{p}|^4} \to \frac{1}{|\mathbf{k}-\mathbf{p}|^4}\frac{|\mathbf{k}-\mathbf{p}|^2}{\kappa^2 + |\mathbf{k}-\mathbf{p}|^2}\,, \tag{A.5}$$

where κ is the screening scale in Eq. (5). Thus one obtains

$$\Gamma_{\gamma\to a} = g_{a\gamma}^2 \frac{T\kappa^2}{32\pi^2}\frac{|\mathbf{p}|}{E}\int d\Omega_p \frac{|\mathbf{k}\times\mathbf{p}|^2}{|\mathbf{k}-\mathbf{p}|^2(\kappa^2 + |\mathbf{k}-\mathbf{p}|^2)}\,, \tag{A.6}$$

and after an integration over the scattering angle we obtain Eq. (4).

Appendix B. ALP production rate from photon coalescence

In order to obtain the ALP production rate from photon coalescence, let us consider the Boltzmann equation for the ALP distribution function f_a

$$\begin{aligned}\frac{\partial f_a}{\partial t} = \frac{1}{2E}\int &\frac{d^3\mathbf{k_1}}{(2\pi)^3 2\omega_1}\frac{d^3\mathbf{k_2}}{(2\pi)^3 2\omega_2} \\ &(2\pi)^4\delta^4(P - K_1 - K_2)\frac{1}{2}|\overline{\mathcal{M}}|^2 \\ &\left[(f_a+1)f_\gamma f_\gamma - f_a(f_\gamma+1)(f_\gamma+1)\right],\end{aligned} \tag{B.1}$$

where $P = (E, \mathbf{p})$ is the ALP 4-momentum, $K_i = (\omega_i, \mathbf{k_i})$ for $i = 1, 2$ are the 4-momenta of the two photons, and $|\overline{\mathcal{M}}|^2$ is the polarization-summed squared matrix element

$$|\overline{\mathcal{M}}|^2 = \frac{1}{2}g_{a\gamma}^2 m_a^2\left[m_a^2 - 4m_\gamma^2\right]. \tag{B.2}$$

The first term in Eq. (B.1) describes the photon coalescence, while the second one is the decay process. Since one can assume that ALPs, once produced by photon coalescence, escape immediately, then $f_a = 0$ and attention can be focused on the photon coalescence term

$$\frac{\partial f_a}{\partial t} = \frac{1}{2E}\int \frac{d^3\mathbf{k_1}}{(2\pi)^3 2\omega_1}\frac{d^3\mathbf{k_2}}{(2\pi)^3 2\omega_2}(2\pi)^4 \delta^4(P - K_1 - K_2)\frac{1}{2}|\overline{\mathcal{M}}|^2 f_\gamma(\omega_1) f_\gamma(\omega_2)\,. \tag{B.3}$$

By integrating, one obtains

$$\frac{\partial f_a}{\partial t} = \frac{g_{a\gamma}^2 m_a}{64\pi E_a}\left[m_a^2 - 4m_\gamma^2\right]^{3/2} e^{-E/T}\,, \tag{B.4}$$

where a Maxwell-Boltzmann distribution for photons is assumed and $\omega_1 + \omega_2 = E$ because of the delta-function. Since

$$dN_a = f_a \frac{d^3\mathbf{p}}{(2\pi)^3} = \frac{f_a\, p\, E\, dE\, d\Omega}{(2\pi)^3}\,, \tag{B.5}$$

the production rate per unit volume of ALPs of energy between E and $E + dE$ results to be

$$\frac{d^2 N_a}{dE\, dt} = \frac{g_{a\gamma}^2}{128\pi^3} m_a^4\, p\left(1 - \frac{4m_\gamma^2}{m_a^2}\right)^{3/2} e^{-E/T}\,. \tag{B.6}$$

References

[1] L. Di Luzio, M. Giannotti, E. Nardi, L. Visinelli, The landscape of QCD axion models, arXiv:2003.01100 [hep-ph].
[2] P. Svrcek, E. Witten, Axions in string theory, J. High Energy Phys. 0606 (2006) 051, https://doi.org/10.1088/1126-6708/2006/06/051, arXiv:hep-th/0605206.
[3] A. Arvanitaki, S. Dimopoulos, S. Dubovsky, N. Kaloper, J. March-Russell, String axiverse, Phys. Rev. D 81 (2010) 123530, https://doi.org/10.1103/PhysRevD.81.123530, arXiv:0905.4720 [hep-th].
[4] M. Cicoli, M. Goodsell, A. Ringwald, The type IIB string axiverse and its low-energy phenomenology, J. High Energy Phys. 1210 (2012) 146, https://doi.org/10.1007/JHEP10(2012)146, arXiv:1206.0819 [hep-th].
[5] P.W. Graham, D.E. Kaplan, S. Rajendran, Cosmological relaxation of the electroweak scale, Phys. Rev. Lett. 115 (22) (2015) 221801, https://doi.org/10.1103/PhysRevLett.115.221801, arXiv:1504.07551 [hep-ph].
[6] Y. Hochberg, E. Kuflik, R. Mcgehee, H. Murayama, K. Schutz, Strongly interacting massive particles through the axion portal, Phys. Rev. D 98 (11) (2018) 115031, https://doi.org/10.1103/PhysRevD.98.115031, arXiv:1806.10139 [hep-ph].
[7] C. Boehm, M.J. Dolan, C. McCabe, M. Spannowsky, C.J. Wallace, J. Cosmol. Astropart. Phys. 1405 (2014) 009, https://doi.org/10.1088/1475-7516/2014/05/009, arXiv:1401.6458 [hep-ph].
[8] M.J. Dolan, T. Ferber, C. Hearty, F. Kahlhoefer, K. Schmidt-Hoberg, Revised constraints and Belle II sensitivity for visible and invisible axion-like particles, J. High Energy Phys. 1712 (2017) 094, https://doi.org/10.1007/JHEP12(2017)094, arXiv:1709.00009 [hep-ph].
[9] D. Cadamuro, S. Hannestad, G. Raffelt, J. Redondo, Cosmological bounds on sub-MeV mass axions, J. Cosmol. Astropart. Phys. 1102 (2011) 003, https://doi.org/10.1088/1475-7516/2011/02/003, arXiv:1011.3694 [hep-ph].
[10] D. Cadamuro, J. Redondo, Cosmological bounds on pseudo Nambu-Goldstone bosons, J. Cosmol. Astropart. Phys. 1202 (2012) 032, https://doi.org/10.1088/1475-7516/2012/02/032, arXiv:1110.2895 [hep-ph].
[11] P.F. Depta, M. Hufnagel, K. Schmidt-Hoberg, Robust cosmological constraints on axion-like particles, arXiv:2002.08370 [hep-ph].
[12] J. Jaeckel, M. Spannowsky, Probing MeV to 90 GeV axion-like particles with LEP and LHC, Phys. Lett. B 753 (2016) 482, https://doi.org/10.1016/j.physletb.2015.12.037, arXiv:1509.00476 [hep-ph].
[13] B. Döbrich, J. Jaeckel, T. Spadaro, Light in the beam dump. Axion-Like Particle production from decay photons in proton beam-dumps, J. High Energy Phys. 1905 (2019) 213, https://doi.org/10.1007/JHEP05(2019)213, arXiv:1904.02091 [hep-ph].
[14] F. Bergsma, et al., CHARM Collaboration, Phys. Lett. B 157 (1985) 458–462, https://doi.org/10.1016/0370-2693(85)90400-9.
[15] J. Blümlein, J. Brunner, Phys. Lett. B 701 (2011) 155–159, https://doi.org/10.1016/j.physletb.2011.05.046, arXiv:1104.2747 [hep-ex].
[16] J. Blümlein, J. Brunner, Beam-dump data, Phys. Lett. B 731 (2014) 320–326, https://doi.org/10.1016/j.physletb.2014.02.029, arXiv:1311.3870 [hep-ph].
[17] M.W. Krasny, et al., Recent searches for short-lived pseudoscalar bosons in electron beam-dumps, in: Contribution to EPS, 1987.
[18] B. Döbrich, CERN Proc. 1 (2018) 253, https://doi.org/10.23727/CERN-Proceedings-2018-001.253, arXiv:1708.05776 [hep-ph].
[19] G.G. Raffelt, D.S.P. Dearborn, Bounds on hadronic axions from stellar evolution, Phys. Rev. D 36 (1987) 2211, https://doi.org/10.1103/PhysRevD.36.2211.
[20] G.G. Raffelt, Astrophysical axion bounds, Lect. Notes Phys. 741 (2008) 51, https://doi.org/10.1007/978-3-540-73518-2_3, arXiv:hep-ph/0611350.
[21] A. Ayala, I. Domínguez, M. Giannotti, A. Mirizzi, O. Straniero, Revisiting the bound on axion-photon coupling from Globular Clusters, Phys. Rev. Lett. 113 (19) (2014) 191302, https://doi.org/10.1103/PhysRevLett.113.191302, arXiv:1406.6053 [astro-ph.SR].
[22] O. Straniero, A. Ayala, M. Giannotti, A. Mirizzi, I. Dominguez, Axion-photon coupling: astrophysical constraints, https://doi.org/10.3204/DESY-PROC-2015-02/straniero-oscar.
[23] M. Giannotti, I. Irastorza, J. Redondo, A. Ringwald, Cool WISPs for stellar cooling excesses, J. Cosmol. Astropart. Phys. 05 (2016) 057, https://doi.org/10.1088/1475-7516/2016/05/057, arXiv:1512.08108 [astro-ph.HE].
[24] M. Giannotti, I.G. Irastorza, J. Redondo, A. Ringwald, K. Saikawa, Stellar recipes for axion hunters, J. Cosmol. Astropart. Phys. 10 (2017) 010, https://doi.org/10.1088/1475-7516/2017/10/010, arXiv:1708.02111 [hep-ph].
[25] V. Anastassopoulos, et al., CAST Collaboration, New CAST limit on the axion-photon interaction, Nat. Phys. 13 (2017) 584–590, https://doi.org/10.1038/nphys4109, arXiv:1705.02290 [hep-ex].
[26] G.G. Raffelt, Stars as Laboratories for Fundamental Physics: The Astrophysics of Neutrinos, Axions, and Other Weakly Interacting Particles, Univ. Pr., Chicago, USA, 1996, 664 pp.
[27] G. Raffelt, D. Seckel, Bounds on exotic particle interactions from SN 1987A, Phys. Rev. Lett. 60 (1988) 1793, https://doi.org/10.1103/PhysRevLett.60.1793.
[28] O. Straniero, I. Dominguez, L. Piersanti, M. Giannotti, A. Mirizzi, The initial mass–final luminosity relation of type II supernova progenitors: hints of new physics?, Astrophys. J. 881 (2) (2019) 158, https://doi.org/10.3847/1538-4357/ab3222, arXiv:1907.06367 [astro-ph.SR].
[29] L. Di Lella, A. Pilaftsis, G. Raffelt, K. Zioutas, Search for solar Kaluza-Klein axions in theories of low scale quantum gravity, Phys. Rev. D 62 (2000) 125011, https://doi.org/10.1103/PhysRevD.62.125011, arXiv:hep-ph/0006327.
[30] G.G. Raffelt, G.D. Starkman, Stellar energy transfer by keV mass scalars, Phys. Rev. D 40 (1989) 942, https://doi.org/10.1103/PhysRevD.40.942.
[31] T. Fischer, The role of medium modifications for neutrino-pair processes from nucleon-nucleon bremsstrahlung - impact on the protoneutron star deleptonization, Astron. Astrophys. 593 (2016) A103, https://doi.org/10.1051/0004-6361/201628991, arXiv:1608.05004 [astro-ph.HE].
[32] G. Lucente, P. Carenza, T. Fischer, M. Giannotti, A. Mirizzi, Heavy axion-like particles and core-collapse supernovae: constraints and impact on the explosion mechanism, arXiv:2008.04918 [hep-ph].
[33] A. Payez, C. Evoli, T. Fischer, M. Giannotti, A. Mirizzi, A. Ringwald, Revisiting the SN1987A gamma-ray limit on ultralight axion-like particles, J. Cosmol. Astropart. Phys. 02 (2015) 006, https://doi.org/10.1088/1475-7516/2015/02/006, arXiv:1410.3747 [astro-ph.HE].
[34] J.S. Lee, Revisiting supernova 1987A limits on axion-like-particles, arXiv:1808.10136 [hep-ph].
[35] Fatih Ertas, Felix Kahlhoefer, On the interplay between astrophysical and laboratory probes of MeV-scale axion-like particles, arXiv:2004.01193 [hep-ph].
[36] P. Carenza, T. Fischer, M. Giannotti, G. Guo, G. Martínez-Pinedo, A. Mirizzi, Improved axion emissivity from a supernova via nucleon-nucleon bremsstrahlung, J. Cosmol. Astropart. Phys. 10 (10) (2019) 016, https://doi.org/10.1088/1475-7516/2019/10/016, arXiv:1906.11844 [hep-ph].
[37] W. DeRocco, P.W. Graham, D. Kasen, G. Marques-Tavares, S. Rajendran, Phys. Rev. D 100 (7) (2019) 075018, https://doi.org/10.1103/PhysRevD.100.075018, arXiv:1905.09284 [hep-ph].
[38] J.D. Bjorken, et al., Search for neutral metastable penetrating particles produced in the SLAC beam dump, Phys. Rev. D 38 (1988) 3375, https://doi.org/10.1103/PhysRevD.38.3375.
[39] A. Berlin, N. Blinov, G. Krnjaic, P. Schuster, N. Toro, Dark matter, millicharges, axion and scalar particles, gauge bosons, and other new physics with LDMX, Phys. Rev. D 99 (7) (2019) 075001, https://doi.org/10.1103/PhysRevD.99.075001, arXiv:1807.01730 [hep-ph].
[40] Private communication with Mauro Raggi.
[41] D.S.M. Alves, N. Weiner, A viable QCD axion in the MeV mass range, J. High Energy Phys. 1807 (2018) 092, https://doi.org/10.1007/JHEP07(2018)092, arXiv:1710.03764 [hep-ph].
[42] G.G. Raffelt, Astrophysical axion bounds diminished by screening effects, Phys. Rev. D 33 (1986) 897.